Supplementary Information

Biogenic FeS nanoparticles modulate the extracellular electron transfer and schwertmannite transformation

Changdong Ke [a], Siyu Zhang [a], Chuling Guo [a, b, *], Yanping Deng [a], Yuancheng Li [a], Qian Yao [a], Xiaohu Jin [a], Zhi Dang [a, b, c]

[a] School of Environment and Energy, South China University of Technology, Guangzhou, 510006, China

[b] The Key Laboratory of Pollution Control and Ecosystem Restoration in Industry Clusters, Ministry of Education, Guangzhou, 510006, China

[c] Guangdong Provincial Key Laboratory of Solid Wastes Pollution Control and Recycling, South China University of Technology, Guangzhou, 510006, China

[*]Corresponding authors: School of Environment and Energy, South China University of Technology, Guangzhou 510006, P.R. China; Tel: +86-20-39380508, Fax: +86-20-39380508

E-mail addresses: clguo@scut.edu.cn (Chuling Guo).

Text S1: Preparation of schwertmannite (Sch)

Sch was precipitated from a ferrous sulfate solution using the H_2O_2 method as described previously. [1] Briefly, 5 mL of H_2O_2 (30%) and 10 g of $FeSO_4 \cdot 7H_2O$ were added to 1 L of deionized water at 25°C and incubated for 24 h. The resultant ochre-colored precipitates were frequently washed with deionized water until the supernatant specific conductance was below 5 μs/cm and then they were freeze-dried.

Text S2: Composition of the modified medium

The modified medium contained (g/L): 0.1 KH_2PO_4, 1.0 NH_4Cl, 0.1 $CaCl_2$, 0.5 $MgCl \cdot 6H_2O$, 5.6 sodium lactate (60%), 4.76 HEPES (4-(2- hydroxyethyl)-1-piperazine ethyl sulfonic acid) and trace elements (1 mL). Trace elements were prepared as described by Myers and Nealson. [2] The medium was sterilized for 30 min at 121°C and cooled down before experiment.

Text S3: Sample analyses

Fe^{2+} concentrations were analyzed through the 1,10-phenanthroline method, using an ultraviolet-visible spectrophotometer (UV-160A, Shimadzu, Japan). [3] Ion chromatography (DIONEX ICS-1500, 148 Sunnyvale, USA) was applied to determine SO_4^{2-} concentration. Lactate and acetate concentrations were determined using High performance liquid chromatography (HPLC, Agilent LC 1260, USA). [4]

Solid-phase samples were rinsed once with deoxygenated deionized water, dried and preserved under anoxic conditions until further analysis. X-ray diffraction (XRD) with Cu Kα radiation (Bruker Advance D8, Germany) was applied to analyze the changes in mineral phases at the end of the incubation. Samples were scanned with a 0.05° 2θ step-size and 2 s count time from 10° ~ 80° 2θ. The morphology of secondary minerals was identified by scanning electron microscope (SEM) (ZEISS Merlin3700, Germany). Transmission electron microscopy (TEM; FEI Talos F200X and Hitachi HT7700 Hitachi H-7000FA 100Kv) required with energy dispersive spectroscopy (EDS; Oxford X-Max) was used to observe the morphology and distribution of the solid phase and bacteria.

Text S4: The qPCR reaction system and procedure

The qPCR reaction system and procedure were as described by Ke et al. [5] The reactions were performed in a total volume of 20 μL with 10 μL 2x SYBR Green

qPCR Master Mix and 0.4 μl ROX Reference Dye (APExBIO, Houston, USA), 0.5 μL each primer (10 μM), and 1 μL of DNA template. The procedures were 95°C initial denaturation 2 min, 40 cycles of 95°C denaturation 15 s, and 60°C annealing 30 s. The melting curve was obtained by heating the sample from 60°C to 95°C. Every sample was measured in triplicate to guarantee the accuracy.

Table S1 Primers used in this study

Primer	Sequence (5'-3')	Amplicon Size (bp)	Reference
recA-F	GTGATGAGGTGGTTGGTAACGAGAC	117	[5]
recA-R	CGCCAGTACGGTTGATACCTTGAC		
mtrC-F	ATGGTGCACCTATGGTCACTG	150	[5]
mtrC-R	AGCCTAAGCCTTGCCAGTTAG		
cymA-F	GCGAAATATTCCATCCTAGCGC	152	[5]
cymA-R	GCCAGCACTTCATTCTTCAAGG		
omcA-F	ATGCCAAGAAAGAACCCG	115	[5]
omcA-R	TGGTCTACTAAACAAGTGTCGC		
phsA-F	ATGTGGTCAGCGGGTGGAATTTATC	103	This study
phsA-R	GCATTGGGTTGGTACGGGACATC		

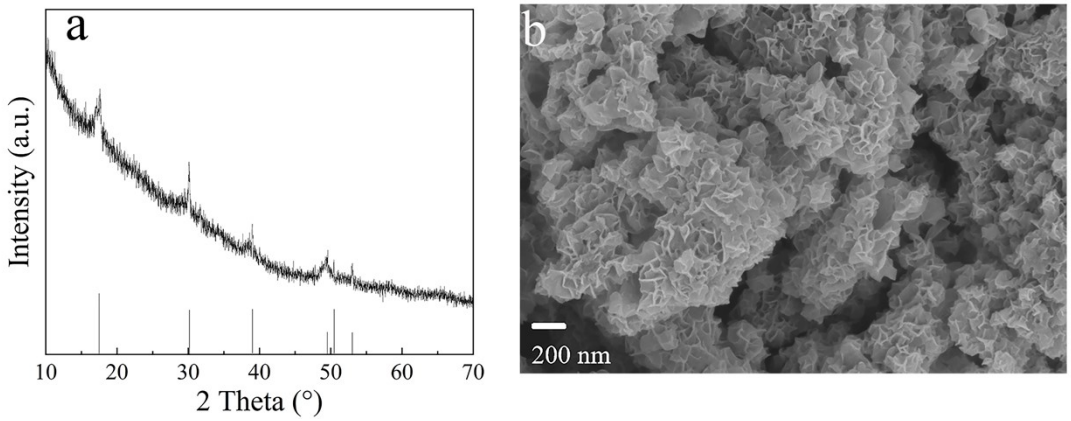

Fig. S1 XRD (a) and SEM images (b) of the FeS NPs.

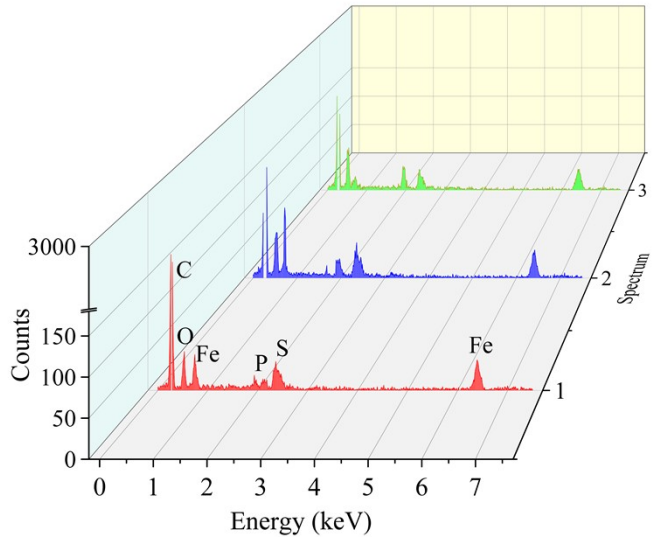

Fig. S2 Determination of element distribution of minerals on cell surface by EDS. The number on the *Z*-axis corresponds to the number in Fig. 1e.

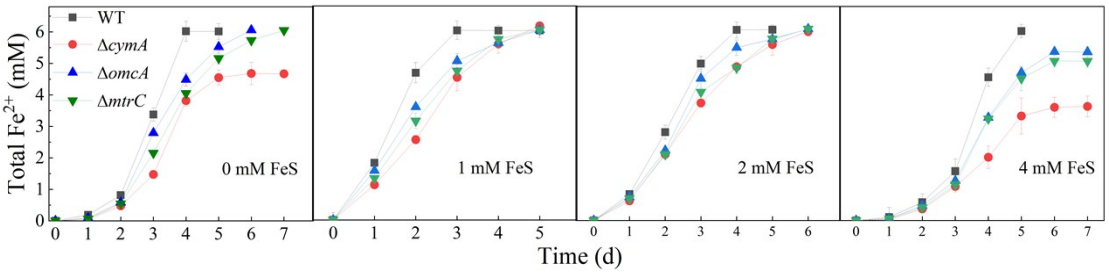

Fig. S3 The total Fe^{2+} concentration during the Sch reduction by *S. oneidensis* MR-1 (WT) and its mutants.

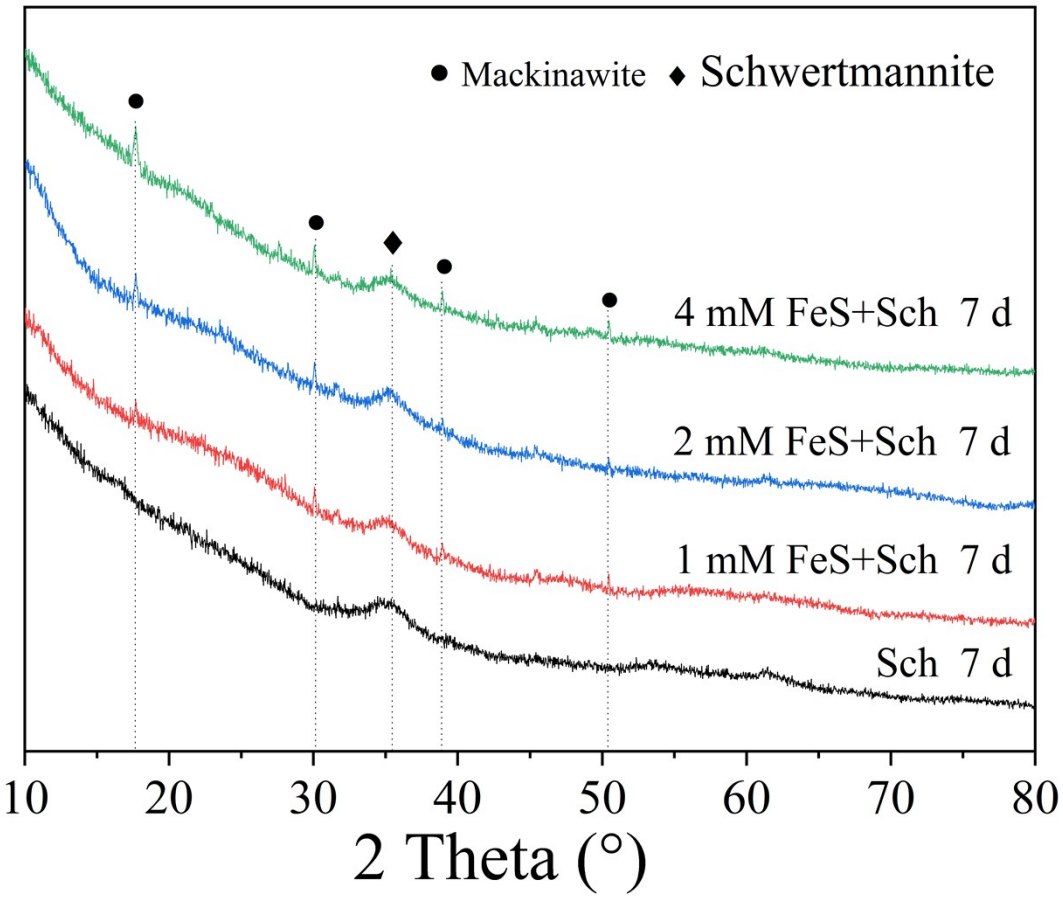

Fig. S4 The interaction of FeS and Sch in the absence of *S. oneidensis* MR-1.

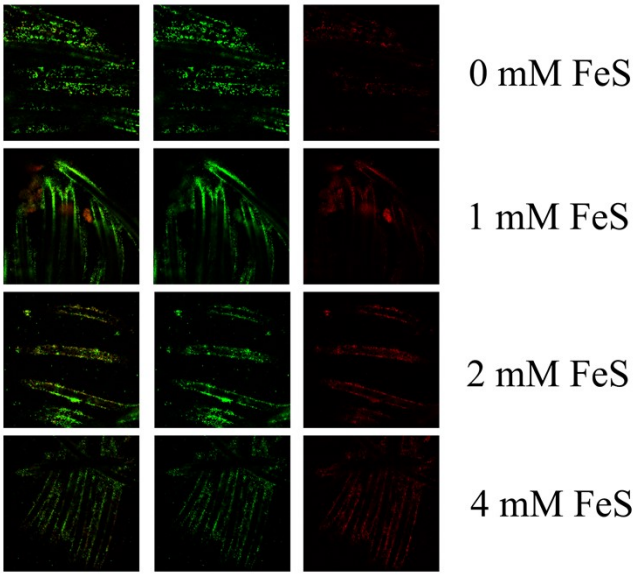

Fig. S5 The cell viability was detected by CLSM.

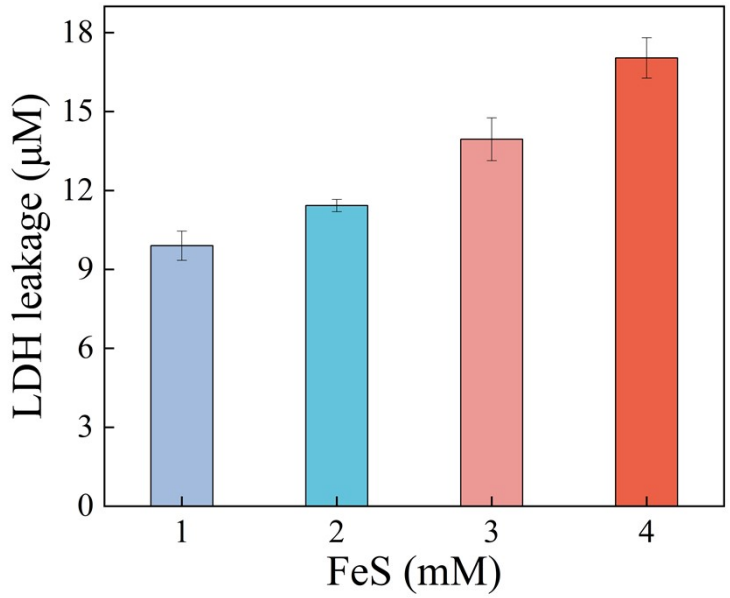

Fig. S6 The cell viability was detected by LDH leakage.

Reference

1. S. Regenspurg, A. Brand and S. Peiffer, Formation and stability of schwertmannite in acidic mining lakes 11Associate editor: C. M. Eggleston, *Geochim. Cosmochim. Ac.*, 2004, **68**, 1185-1197.
2. C. R. Myers and K. H. Nealson, Bacterial manganese reduction and growth with manganese oxide as the sole electron acceptor, *Science*, 1988, **240**, 1319-1321.
3. N. Brand, G. Mailhot and M. Bolte, Degradation photoinduced by Fe (III): method of alkylphenol ethoxylates removal in water, *Environ. Sci. Technol.*, 1998, **32**, 2715-2720.
4. D. B. Albert and C. S. Martens, Determination of low-molecular-weight organic acid concentrations in seawater and pore-water samples via HPLC, *Mar. Chem.*, 1997, **56**, 27-37.
5. C. Ke, C. Guo, S. Zhang, Y. Deng, X. Li, Y. Li, G. Lu, F. Ling and Z. Dang, Microbial reduction of schwertmannite by co-cultured iron-and sulfate-reducing bacteria, *Sci. Total Environ.*, 2023, **861**, 160551.